# Xenon doping studies in ProtoDUNE-DP

J. Soto on behalf of CIEMAT team

December 18th 2020

# Content

- Xe and N2 doping in ProtoDUNE-DP.
- Impact on the light yield at different triggers.
- Scintillation time profile:
  - PEN / TPB differences.
  - Fitting to a model.
  - SP-DP comparison.

# Summary of the DP re-filling and $N_2$ injections

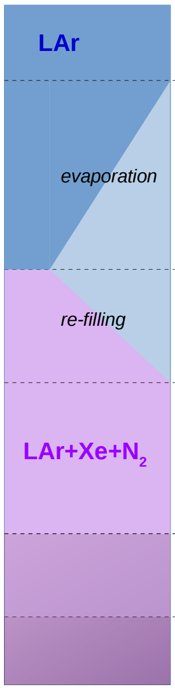


- May 6th - ProtoDUNE Dual-Phase re-circulation system was stopped, to allow to reduce the LAr level and fix the HV extender.
- July 22nd – Re-filling starts: LAr + Xe (5.7 ppmv ,18.8pmmm)+ N2 (5.6 ppmv) from ProtoDUNE-SP starts entering the cryostat.
- July 23rd – Re-filling ends: LAr + Xe (5.8pmmm) + N2 (~1.7 ppmv)
- August 3rd – 3cm more: LAr + Xe (5.9pmmm) + N2 (~1.7 ppmv)
- August 14th – 1st injection of $N_2$: LAr + Xe (5.8pmmm) + N2 (~2.7 ppmv)
- August 28th – 2nd injection of $N_2$: LAr + Xe (5.8pmmm) + N2 (~4.7 ppmv)

(From the last collaboration meeting)

# Impact on the light yield

## Trigger comparison

CRT Trigger

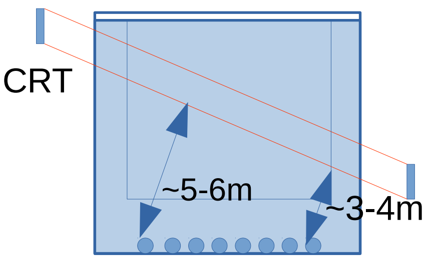


PMT Trigger

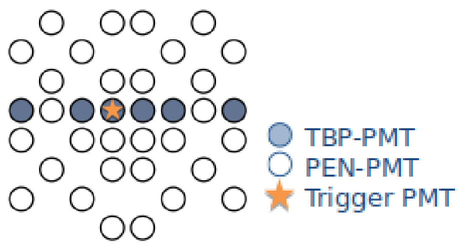


Charge integration:

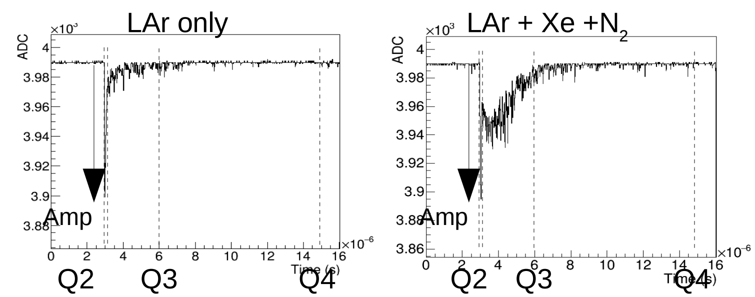


**Relative variation of the average signal detected at different triggers:**

Error show STD variation among PMTs.

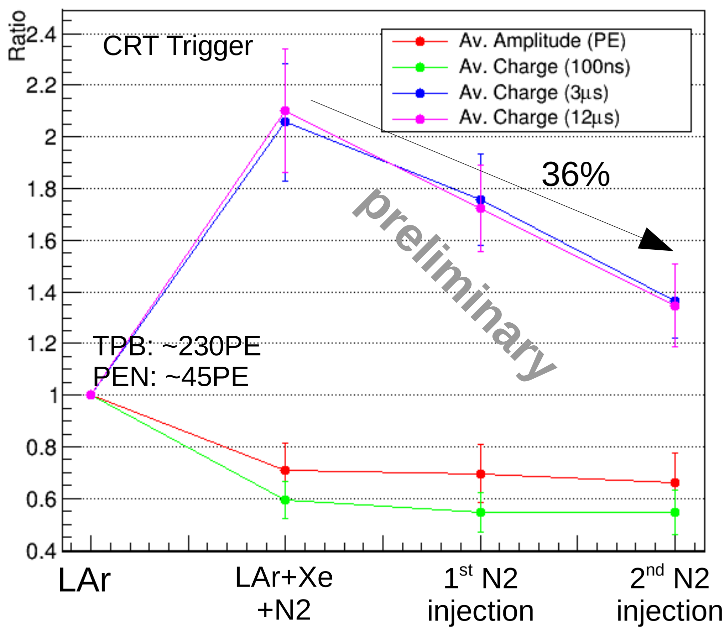


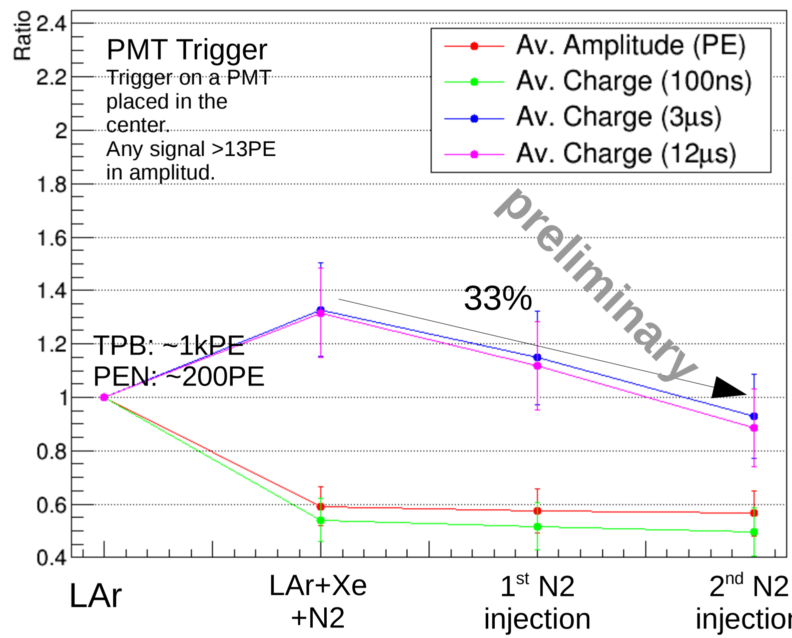


In these runs the detector is always full of liquid.

# Light monitoring during evaporation, filling and doping. CRT Trigger

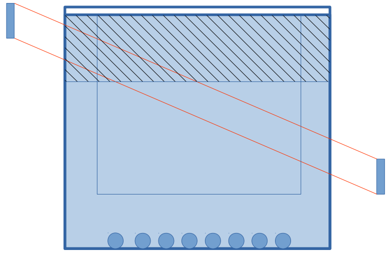

PMTs have been taking data during the evaporation, refilling with LAr+Xe+N2 and N2 injections in order to monitor the light changes.

**Relative variation of the average signal detected in CRT trigger runs by all PMTs.**
Error show STD variation among PMTs.

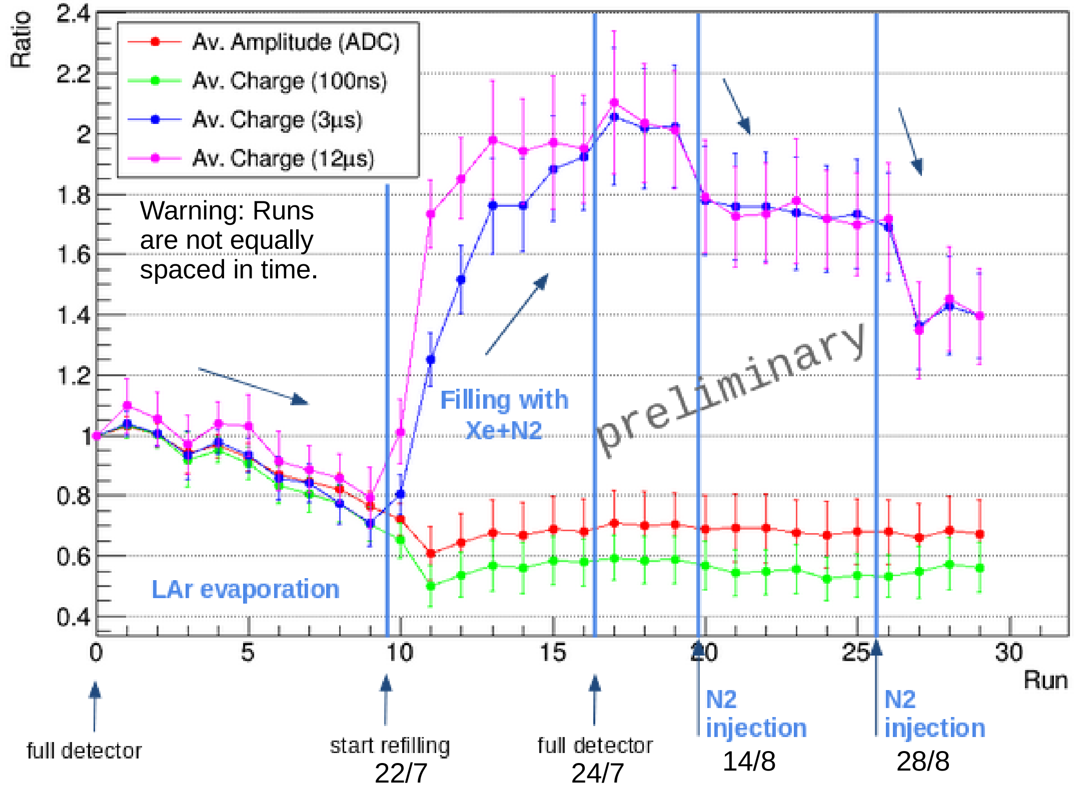


- Light yield decreases as the liquid level goes down and part of the muon track is out of the liquid.
- During the refilling the light yield is recovered but the amplitude is still below the value with the detector filled.
- N2 injections reduce the light yield but keeps the amplitude at a similar level.

# Light monitoring during evaporation, filling and doping. PMT Trigger

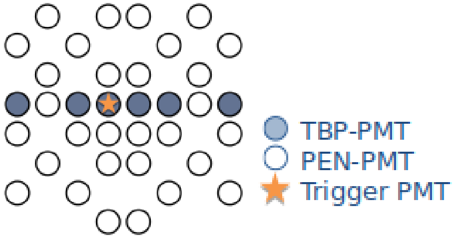


**Relative variation of the average signal detected in PMT trigger runs (signals>13PEs ina PMT at the center):**
Error show STD variation among PMTs.

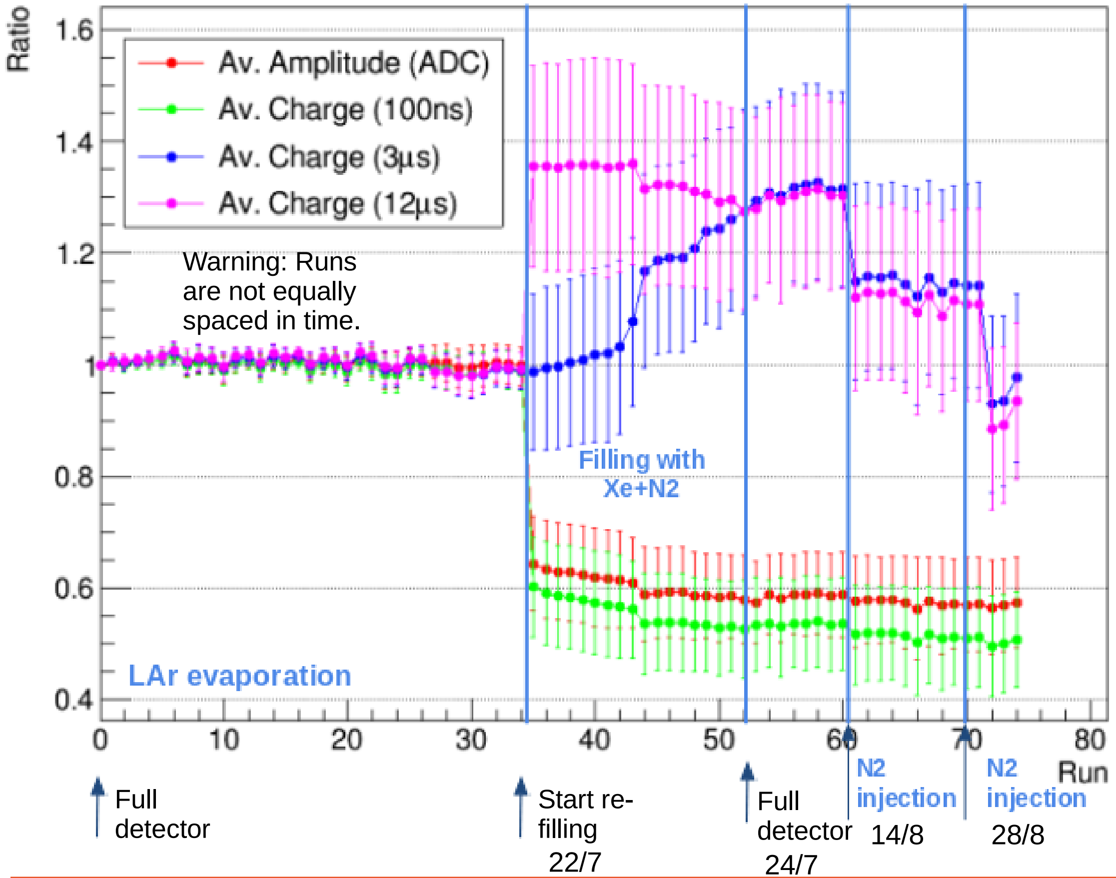


- Light level is stable during evaporation: This is consistent with having tracks close to the PMTs in this trigger.
- We see most of the fall in the amplitude right in the beginning of the filling (with Xe and N2 concentrations still very low).
- N2 injections reduce the light yield but keeps the amplitude at a similar level.
- All PMTs are averaged. Large errors are due to the dependence of the detected light on each PMT with the distance to the trigger PMT. A more detail analysis is ongoing.

# Scintillation time profile during re-filling

- Scintillation profile: Average waveform centering  the maximum and substracting baseline.

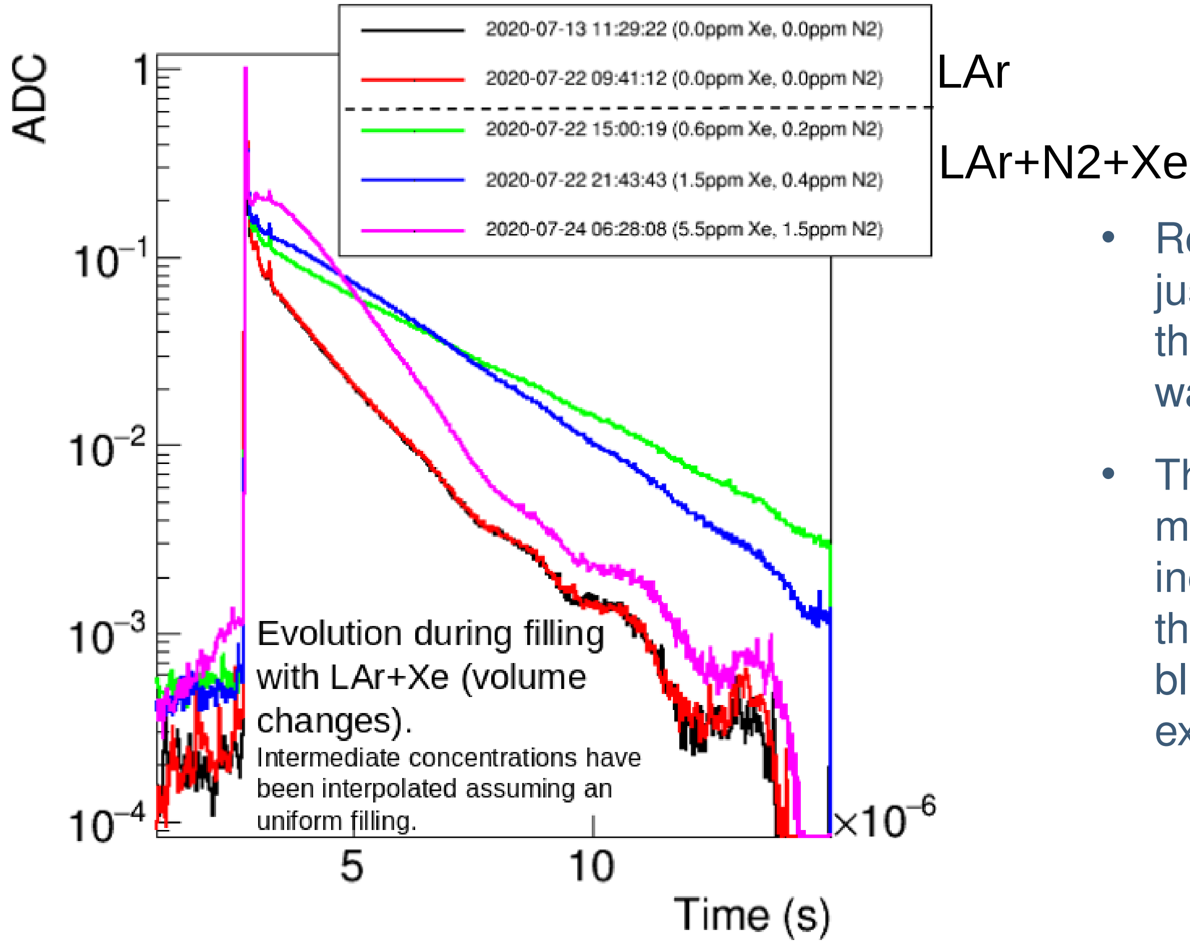


- Red (black) is a run taken just before (one week before) the filling. See how stable it was.
- Then, in the very first moment the tau slow is increased (red to green) and then it shrinks back (green – blue - pink) loosing the exponential shape.

# Scintillation in xenon doped liquid argon + nitrogen

Without dopants, the time profile consist of the sum of two exponentials with different time decay constant. One for the single state (~6ns), and a slower one for the triplet sate (~1.44us):

$$P1\ e^{-t/\tau Fast} + P2\ e^{-t/\tau slow}$$

(all at 128 nm)

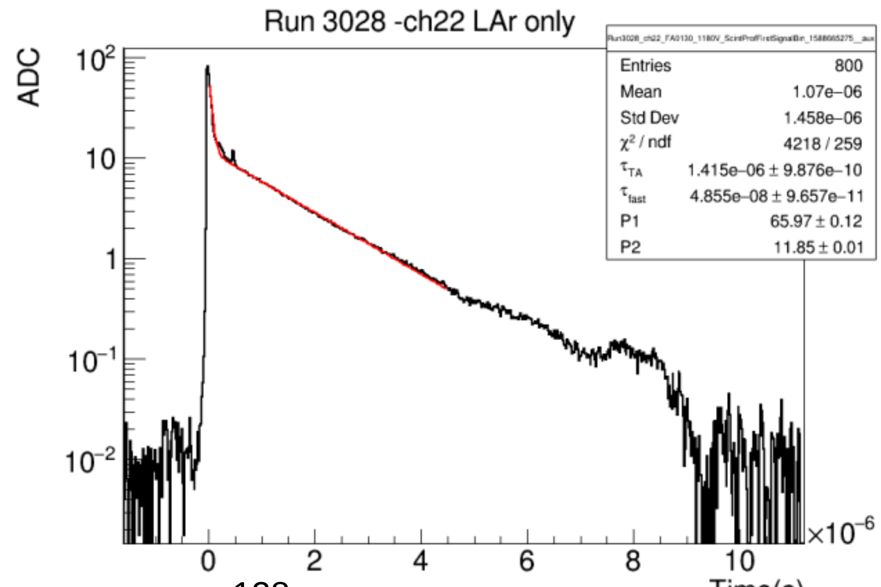


Considering only the Xenon dopants, a model based in three exponentials is provided in the literature, where TA is the energy transfer time from ArAr* to XeXe* for the slow component:
(Fast component is not transferred at our low doping values.)

$$Ar_2^*({}^{1,3}\Sigma_u^+) \rightarrow Ar_2^*({}^{1,3}\Sigma_g^+) + h\nu(128\ \text{nm})$$

$$Ar_2^*({}^{3}\Sigma_u^+) + Xe + (\text{migration}) \rightarrow (ArXe)^* + Ar$$

$$(ArXe)^* + Xe + (\text{migration}) \rightarrow Xe_2^*({}^{1,3}\Sigma_u^+) + Ar$$

$$Xe_2^*({}^{1,3}\Sigma_u^+) \rightarrow 2Xe + h\nu(175\ \text{nm})$$

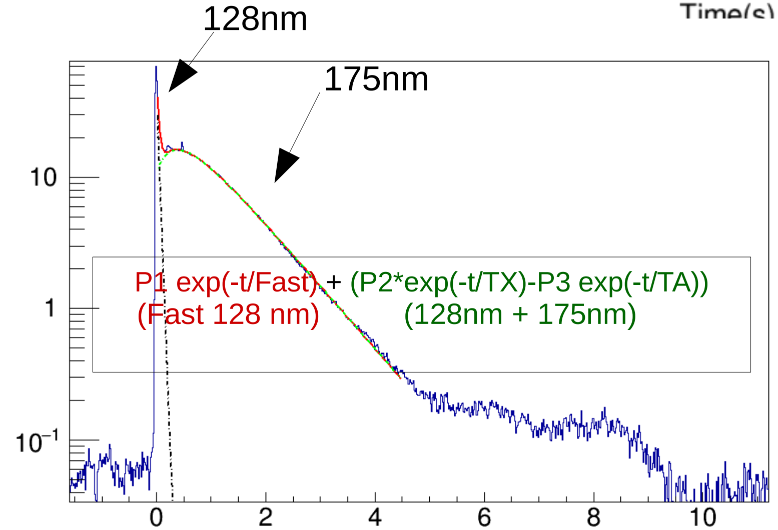


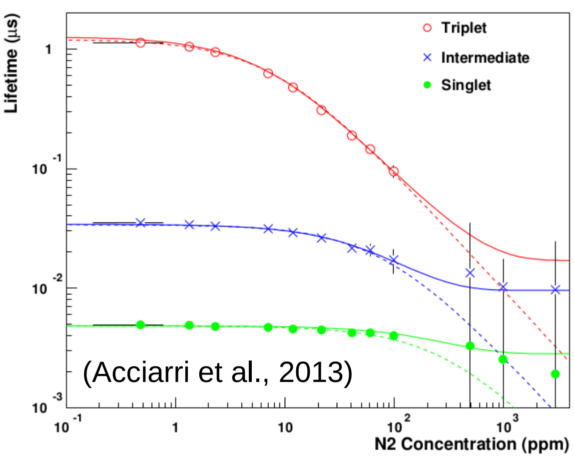


Nitrogen contaminants reduce the triplet decay time.

$$\frac{1}{\tau'_j}([N_2]) = \frac{1}{\tau_j} + k_Q\,[N_2]$$

$k_Q(N_2) = 0.11 \pm 0.01\ \mu s^{-1}\text{ppm}^{-1}$

# Example fit

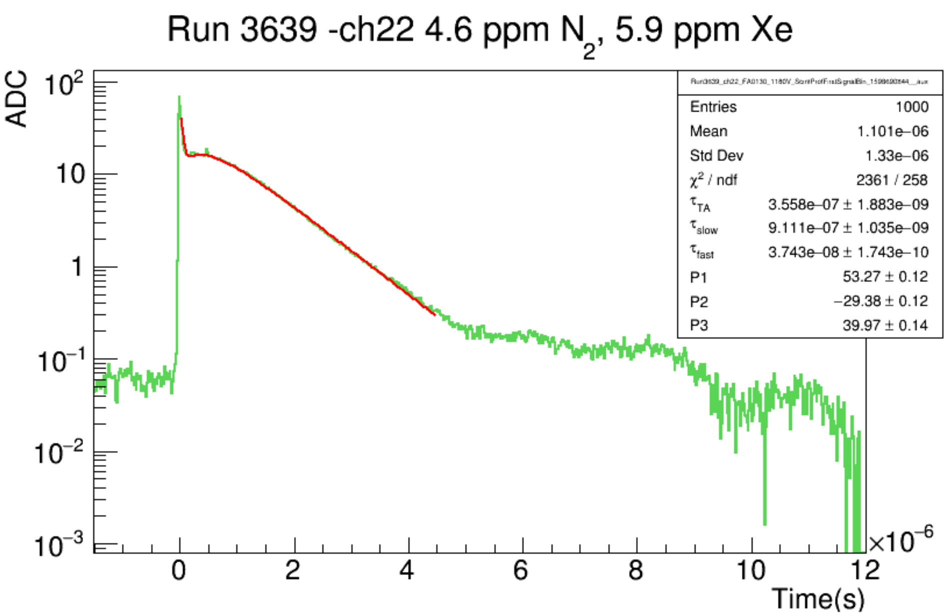


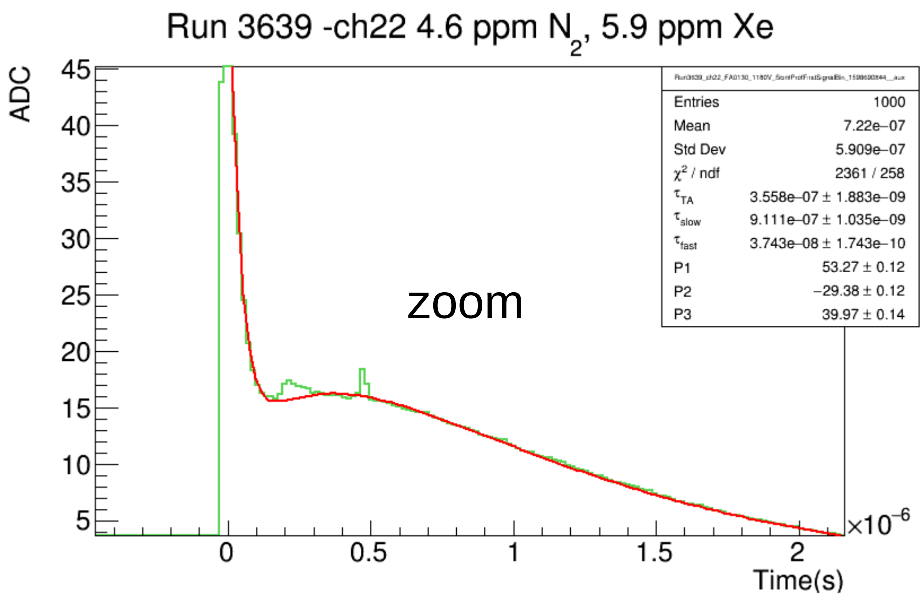


P1 exp(-t/Fast) + P2 exp(-t/Td)+P3 exp(-t/Tslow)
(Fast 128 nm) (128nm+175nm)

Reflexion bins are excluded from the fit.

# PEN TPB differences

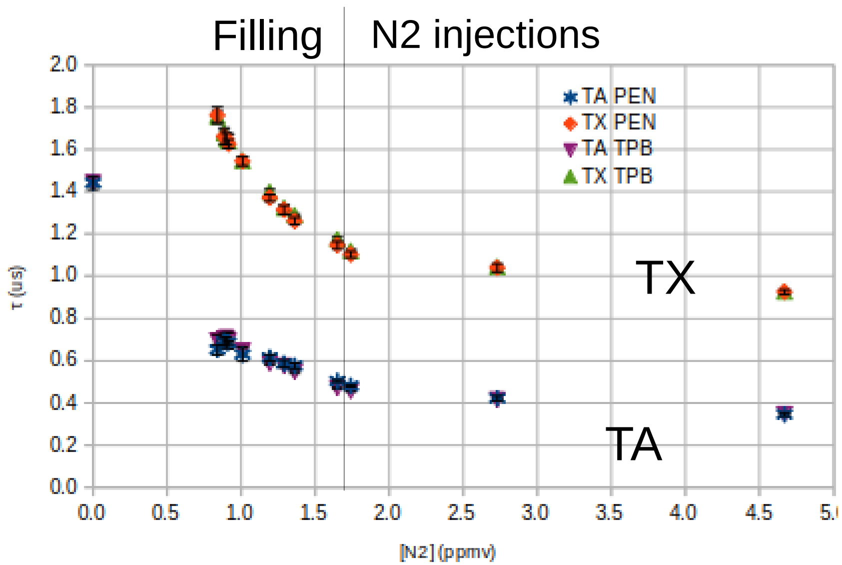


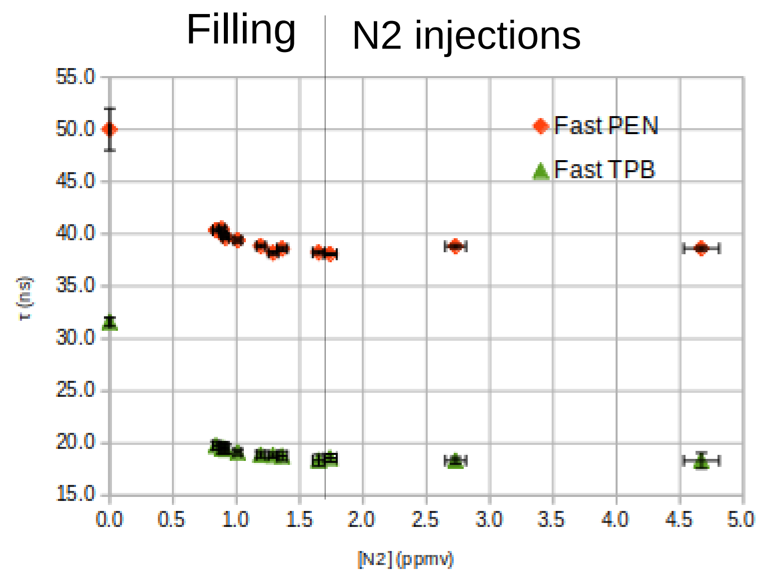


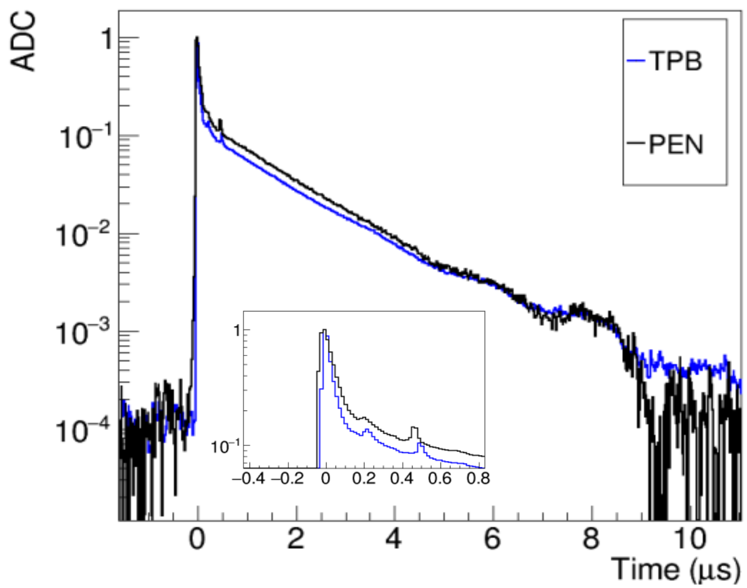


- TA and TX are mostly compatible between PEN and TPB PMTs as expected.
- Fast component is larger on PEN PMTs!
- Fast component seems to decrease with the concentration.

# Model of the time constants:

A. Neumeier et al 2015 EPL109 12001

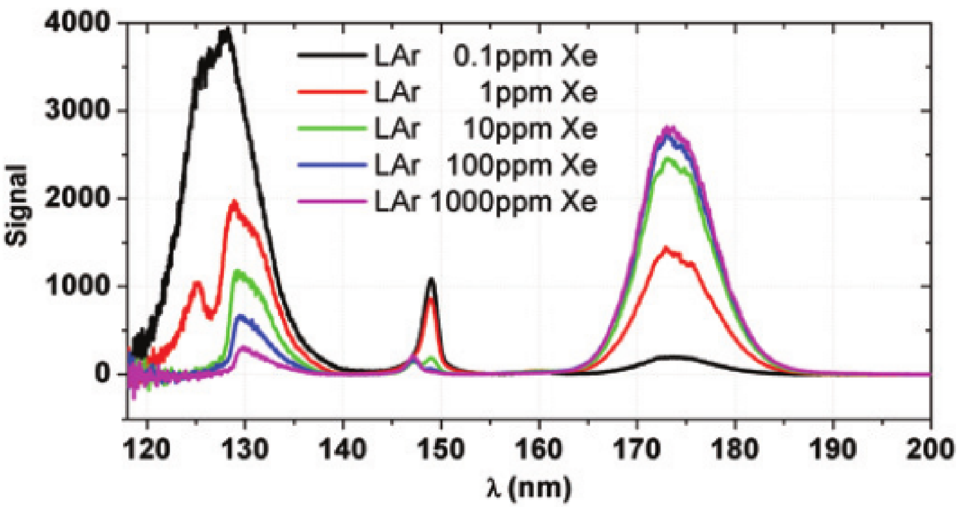


- At low Xe concentrations (which is our case), we also have a significant contribution at 150 nm.
- 3 contributions:
  128, 147 and 175nm

ArAr* → γ (128)

ArAr* + Xe → ArXe* + Ar (**AX**) → γ (150)

ArXe* + Xe → XeXe* + Ar (**XX**)→ γ (175) (much faster)

ArAr* + N2 → ArAr + N2* (**N2,Ar**) (quenching)

ArXe* + N2 → ArXe + N2* (**N2,Xe**) (quenching)

Rate of **ArAr*** deexitation:

$$\frac{dAA}{dt} = -\frac{AA}{\tau_{128}} - \frac{AA}{\tau_{N2}} - \frac{AA}{\tau_{AX}} = -\frac{AA}{\tau_{TA}}$$

Rate of **ArXe*** generation / deexitation:

$$\frac{dAX}{dt} = +\frac{AA}{\tau_{AX}} - \frac{AX}{\tau_{150}} - \frac{AX}{\tau_{N2}} - \frac{AX}{\tau_{XX}} = +\frac{AA}{\tau_{AX}} - \frac{AX}{\tau_{TX}}$$

Rate of **XeXe*** generation / deexitation::

$$\frac{dXX}{dt} = +\frac{AX}{\tau_{XX}} - \frac{XX}{\tau_{175}}$$

Assuming $\tau_{175}$ is very small, the solution to these equations is the sum of two exponentials:

**P2 expo(-t/TA) + P3 expo(-t/TX)**

$$\frac{1}{\tau_{TA}} = \frac{1}{\tau_{128}} + \frac{1}{\tau_{N2}} + \frac{1}{\tau_{AX}}$$

$$\frac{1}{\tau_{TX}} = \frac{1}{\tau_{150}} + \frac{1}{\tau_{N2}} + \frac{1}{\tau_{XX}}$$

1/TA = A [N2] + B [Xe] + C

1/TX =D [N2] + E [Xe] + F

$$\frac{1}{\tau'_j}([N_2]) = \frac{1}{\tau_j} + k_Q\,[N_2]$$

# Linear fit:

**P2 expo(-t/TA) + P3 expo(-t/TX)**

1/TA = A [N2] + B [Xe] + C, with: $\frac{1}{\tau_{TA}} = \frac{1}{\tau_{128}} + \frac{1}{\tau_{N2}} + \frac{1}{\tau_{AX}}$

1/TX = D [N2] + E [Xe] + F $\frac{1}{\tau_{TX}} = \frac{1}{\tau_{150}} + \frac{1}{\tau_{N2}} + \frac{1}{\tau_{XX}}$

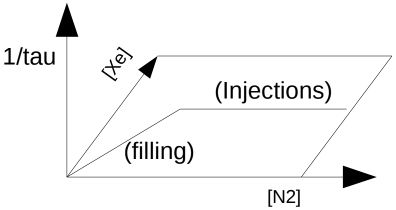


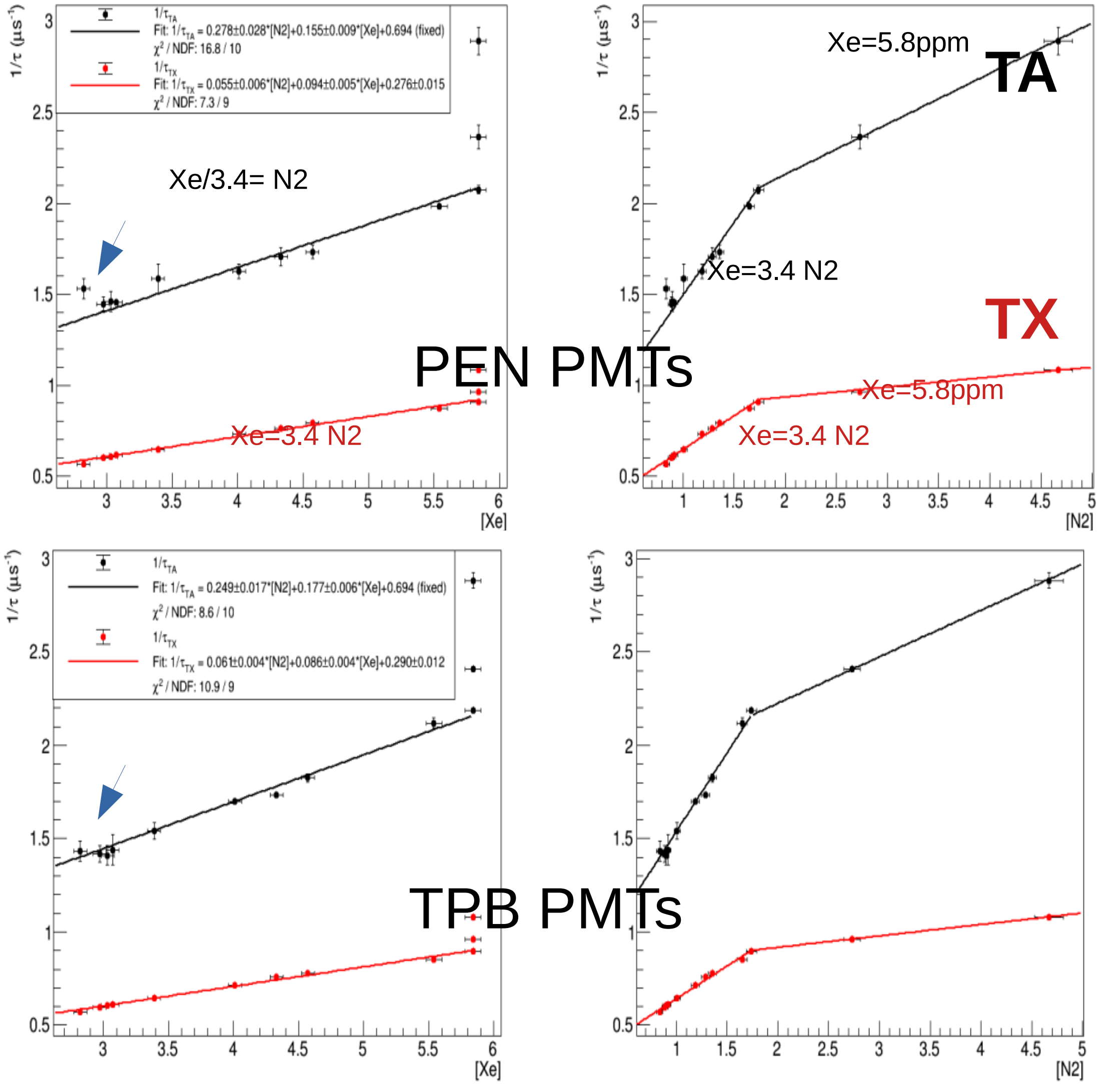


- We obtain similar results on PEN and TPB PMTs.
- Linearity is worse on PEN PMTs at low doping levels (as expected)

| | 12 points | | | | | |
|---|---|---|---|---|---|---|
| | PEN | | TPB | | Difference | |
| Par | Value | Error | Value | Error | Rel | Δ(σ) |
| A | 0.278 | 0.028 | 0.249 | 0.017 | -10% | -0.9 |
| B | 0.155 | 0.009 | 0.177 | 0.006 | 14% | 2.0 |
| C | 0.694 | - | 0.694 | - | 0% | - |
| D | 0.055 | 0.006 | 0.061 | 0.004 | 11% | 0.8 |
| E | 0.094 | 0.005 | 0.086 | 0.004 | -9% | -1.2 |
| F | 0.276 | 0.015 | 0.29 | 0.012 | 5% | 0.7 |

| | 12 points | | | | | |
|---|---|---|---|---|---|---|
| | PEN | | TPB | | Difference | |
| Tau (us) | Value | Error | Value | Error | Rel | Δ(σ) |
| AX (us ppm) | 6.45 | 0.37 | 5.65 | 0.19 | -12% | -1.9 |
| XX (us ppm) | 10.64 | 0.57 | 11.63 | 0.54 | 9% | 1.3 |
| N2,Ar (us ppm) | 3.60 | 0.36 | 4.02 | 0.27 | 12% | 0.9 |
| N2,Xe (us ppm) | 18.18 | 1.98 | 16.39 | 1.07 | -10% | -0.8 |
| 128 (us) | 1.44 | 1.44 | 1.44 | 1.44 | 0% | 0.0 |
| 150 (us) | 3.62 | 0.20 | 3.45 | 0.14 | -5% | -0.7 |

# Linear fit including np04 data (on TPB PMTs):

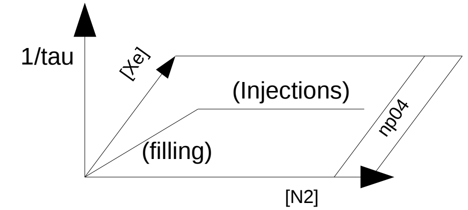


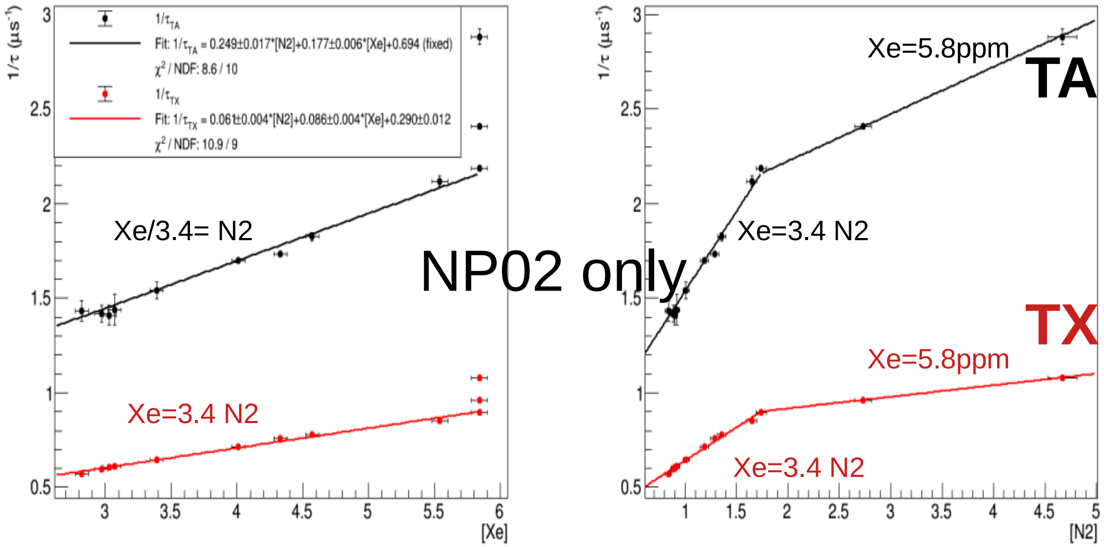


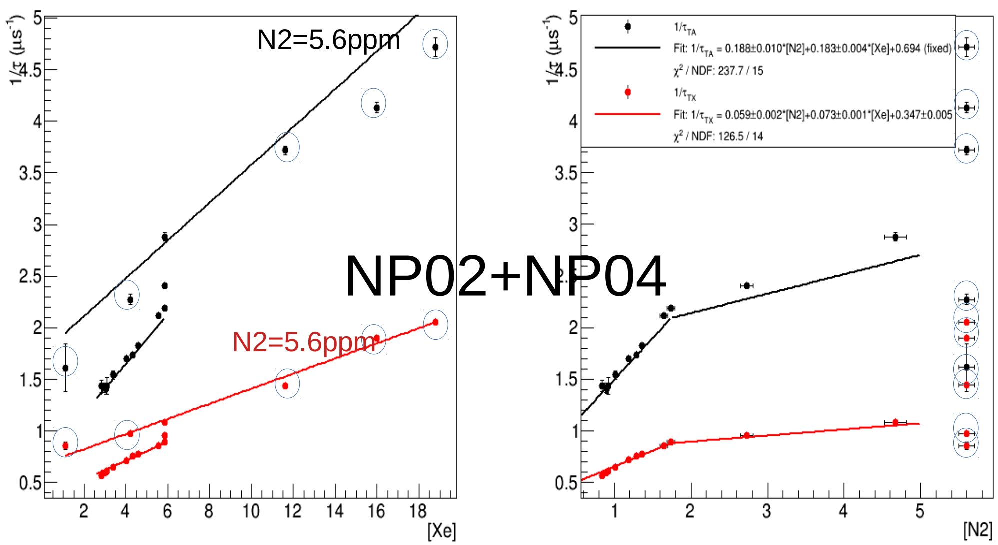


- Including tau values from np04 provided by Francesco (fitting by pairs), points in the circle.

- chi2 gets much worse: From ~1 to ~10.

-Only some parameters are affected:

1/TA = **A** [N2] + **B** [Xe] + C

1/TX = **D** [N2] + **E** [Xe] + **F**

| | 12 RUNS – TPB PMTs | | | | | |
|---|---|---|---|---|---|---|
| | DP | | SP+DP | | Variation | |
| Par | Value | Error | Value | Error | Rel | Δ(σ) |
| A | 0.249 | 0.017 | 0.188 | 0.010 | -24% | -3.1 |
| B | 0.177 | 0.006 | 0.183 | 0.004 | 3% | 0.8 |
| C | 0.694 | - | 0.694 | 0.000 | 0% | - |
| D | 0.061 | 0.004 | 0.059 | 0.002 | -3% | -0.4 |
| E | 0.086 | 0.004 | 0.073 | 0.001 | -15% | -3.2 |
| F | 0.290 | 0.012 | 0.347 | 0.005 | 20% | 4.4 |

| | 12 RUNS | | | | | |
|---|---|---|---|---|---|---|
| | DP | | SP+DP | | Variation | |
| Tau (us) | Value | Error | Value | Error | Rel | Δ(σ) |
| AX (us ppm) | 5.65 | 0.19 | 5.46 | 0.12 | -3% | -0.8 |
| XX (us ppm) | 11.6 | 0.5 | 13.70 | 0.19 | 18% | 3.6 |
| N2,Ar (us ppm) | 4.0 | 0.3 | 5.32 | 0.28 | 32% | 3.3 |
| N2,Xe (us ppm) | 16.4 | 1.1 | 16.95 | 0.57 | 3% | 0.5 |
| 128 (us) | 1.44 | 1.44 | 1.44 | 0.00 | 0% | - |
| 150 (us) | 3.45 | 0.14 | 2.88 | 0.04 | -16% | -3.8 |

# DP vs SP+DP comparison:

- We obtain similar values on 2 parameters: $\tau_{AX}$ and $\tau_{N2}$ on ArXe.

- Larger variation introduced on $\tau_{XX}$,$\tau_{N2}$ on ArAr and $\tau_{150.}$

- Errors in the global fit seems overestimated vs the linear fit → They don't include an error in the doping concentrations.

- No variation in the fitting parameters is found when going from DP+SP to SP. However, the ratio of XX/150 obtained from the Quarz/nonQuarz arapucas is not compatible with the ratio obtained from the taus: 3.3±0.1 (DP) vs 2.4±0.5 (SP)

| | LINEAR | | | | | | | | | |
|---|---|---|---|---|---|---|---|---|---|---|
| | DP only | | | | DP+SP | | SP only | | | |
| | PAR | ERROR | Rel | Δ(σ) | PAR | ERROR | PAR | ERROR | Rel | Δ(σ) |
| AX (us ppm) | 5.6 | 0.2 | 3% | 0.8 | 5.46 | 0.12 | 5.39 | 0.09 | -1% | -0.5 |
| XX (us ppm) | 11.6 | 0.5 | -15% | -3.6 | 13.70 | 0.19 | 13.6 | 0.2 | -1% | -0.3 |
| N2,Ar (us ppm) | 4.0 | 0.3 | -24% | -3.3 | 5.3 | 0.3 | 8.2 | 0.7 | 54% | 4.0 |
| N2,Xe (us ppm) | 16.4 | 1.1 | -3% | -0.5 | 16.9 | 0.6 | 12.4 | 1.0 | -27% | -4.0 |
| 128 (us) | 1.4 | 1.4 | 0% | - | 1.44 | 0.00 | 1.40 | 0.10 | -3% | -0.4 |
| 150 (us) | 3.4 | 0.1 | 20% | 3.8 | 2.88 | 0.04 | 5.6 | 1.0 | 94% | 2.6 |

| | GLOBAL | | | | | | | | | |
|---|---|---|---|---|---|---|---|---|---|---|
| | DP only | | | | DP+SP | | SP only | | | |
| | PAR | ERROR | Rel | Δ(σ) | PAR | ERROR | PAR | ERROR | Rel | Δ(σ) |
| AX (us ppm) | 5.9 | 0.2 | 4% | 1.5 | 5.69 | 0.03 | 5.54 | 0.01 | -3% | -5.4 |
| XX (us ppm) | 11.4 | 0.1 | -15% | -21.7 | 13.40 | 0.04 | 13.61 | 0.01 | 2% | 5.3 |
| N2,Ar (us ppm) | 3.8 | 0.2 | -41% | -15.6 | 6.45 | 0.07 | 6.6±0.4 (me) / 9.8±0.9 (Fr.) | | 2 / 52% | 0.3 / 3.8 |
| N2,Xe (us ppm) | 16.6 | 0.2 | 16% | 8.8 | 14.3 | 0.2 | 10.5 | 0.7 | -26% | -5.5 |
| 128 (us) | 1.4 | - | 0% | - | 1.44 | 0.00 | 1.40 | 0.10 | -3% | -0.4 |
| 150 (us) | 3.5 | 0.1 | 17% | 6.1 | 2.97 | 0.06 | 5.58 | 1.03 | 88% | 2.5 |

XX/150 = 2.4±0.5

# Discrepancy in the fitting results on SP only:

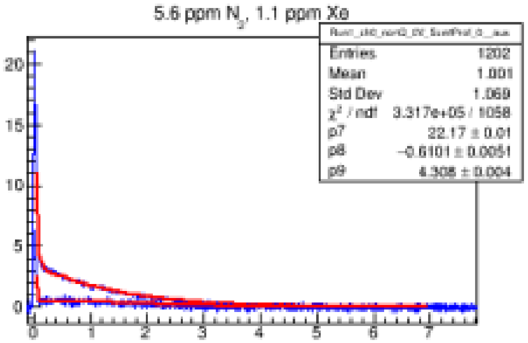


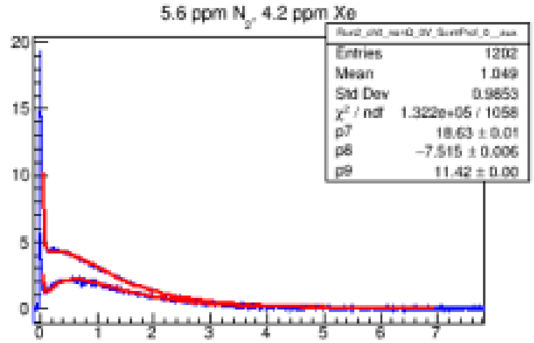


A and D are fixed to zero to remove the dependency with [N2]:

1/TA = ~~A [N2] +~~ B [Xe] + C

1/TX = ~~D [N2] +~~ E [Xe] + F

| (us/ppm) | par | Francesco |
|---|---|---|
| A | 0 | 0 |
| B | 0.181 | 0.180 |
| C | 1.566 | 1.284 |
| D | 0 | 0 |
| E | 0.073 | 0.073 |
| F | 0.713 | 0.723 |
| Tau_Fast | 0.03 | 0 |
| chi2 | 152.12 | |

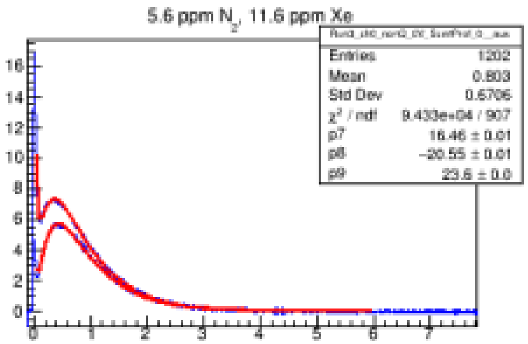


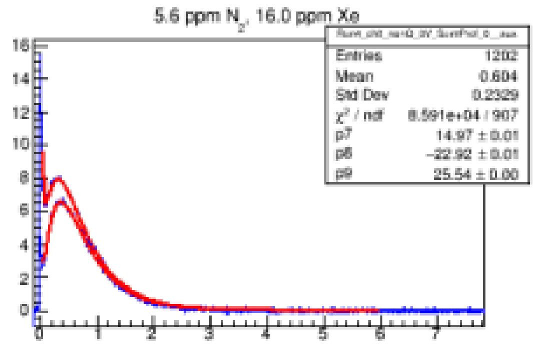


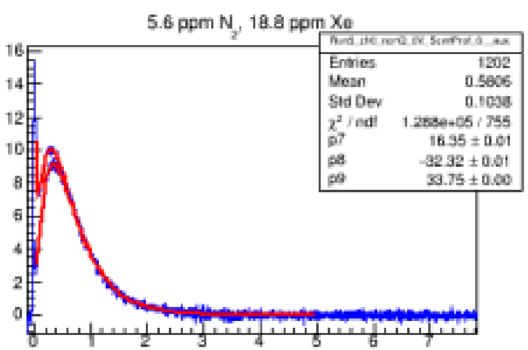


(Francesco)

$$\frac{1}{\tau_{TA}} = A + B\,Xe[ppm]$$

and

$$\frac{1}{\tau_{TX}} = C + D\,Xe[ppm].$$

The global fit provides the values of A, B, C and D together with tau-fast and the coefficients of the exponential functions (three for each plot). The values of A=1.284, B=0.1802, C=0.7225 and D=0.0726 , extracted from the fit, are used in the following calculations to estimate the relevant physical parameters of the Ar to Xe shifting mechanism ($\tau_{AX}$ , $\tau_{XX}$) as well as $\tau_{N2}$ and $\tau_{150}$.

# Including the quenching in the fast component (a la Dante)

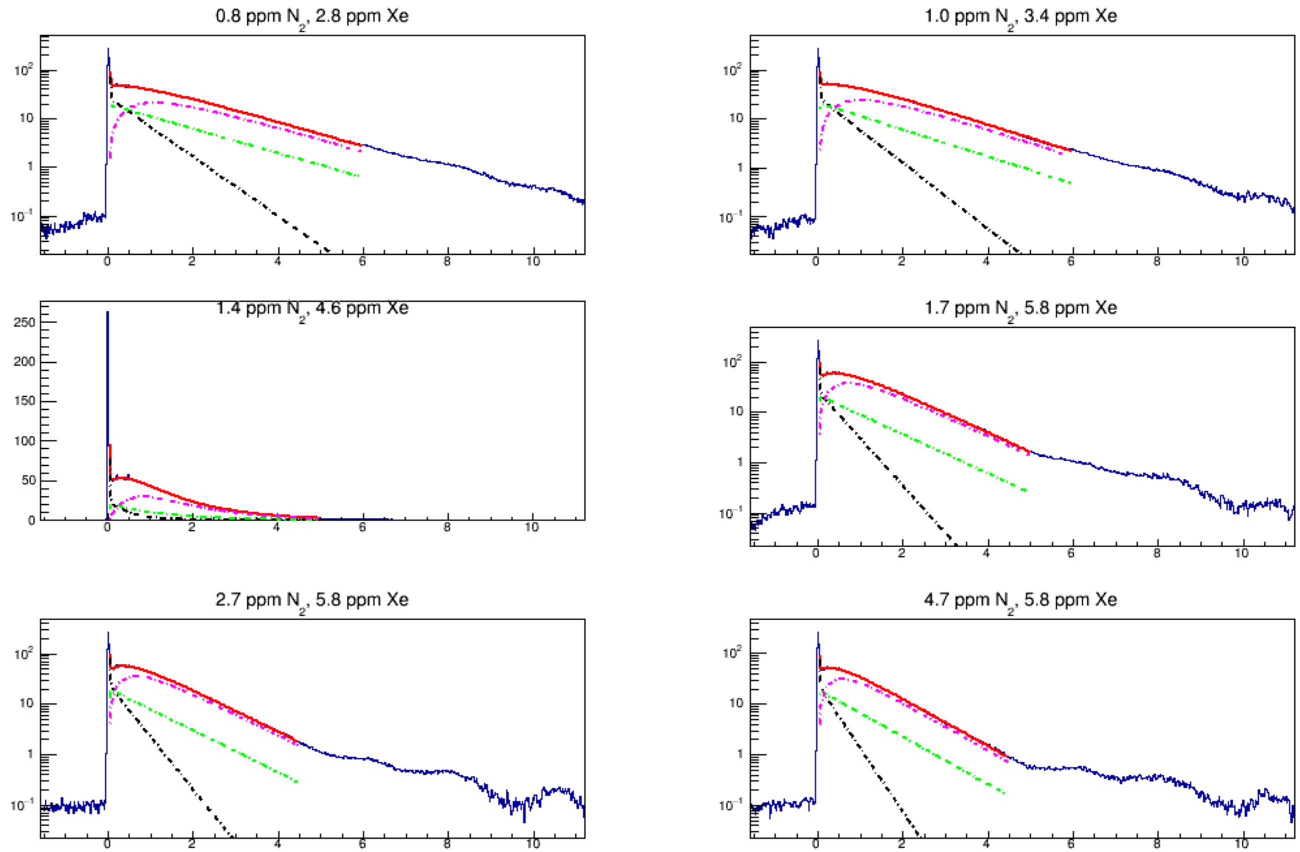


$$F := \mathbf{P1}\ \{e^{(-t/TAFast)} + R*e^{(-t/TASlow)}\} + \mathbf{P2}\ \{e^{(-t/TXFast)} - e^{(-t/TAFast)}\} + \mathbf{P3}\ \{e^{(-t/TXSlow)} - e^{(-t/TASlow)}\}$$

TAFast = A[N2]+**4***B[Xe] + CFast

TXFast = D[N2]+E[Xe] + F

TASlow = A[N2]+B[Xe] + Cslow

TXSlow = D[N2]+E[Xe] + F

| Tau (us) | Standard | | Fast Transfer | | Rel | Δ(σ) |
|---|---|---|---|---|---|---|
| | par | err | par | err | | |
| AX (us ppm) | 5.9 | 0.2 | 5.8 | 0.1 | -2.8% | -0.8 |
| XX (us ppm) | 11.4 | 0.1 | 11.5 | 0.1 | 0.8% | 0.7 |
| N2,Ar (us ppm) | 3.8 | 0.2 | 4.0 | 0.2 | 6.7% | 1.1 |
| N2,Xe (us ppm) | 16.6 | 0.2 | 16.3 | 0.2 | -1.6% | -1.1 |
| 128 (us) | 1.4 | - | 1.44 | - | -% | - |
| 150 (us) | 3.5 | 0.1 | 3.5 | 0.1 | -0.6% | -0.2 |
| 128Fast (us) | 0.0 | 0.0 | 0.020 | 0.000 | | |

We don't get a big variation in the parameters.

# Comparing with the literature

- Wahl provided a parameterization of the time constants:

TA(Wahl) (us) = 2.7 [Xe/ppmm]^(-0.7)

1/TX(Wahl) (us) = 0.51+0.088 [Xe/pmmm]

- We also include the quenching from Acciarri of 0.11/(us ppm) (it doesnt affect much the curves though).

1/TA = 1/TA(Wahl) + 0.11[N2]

1/TX = 1/TX(Wahl) + 0.11[N2]

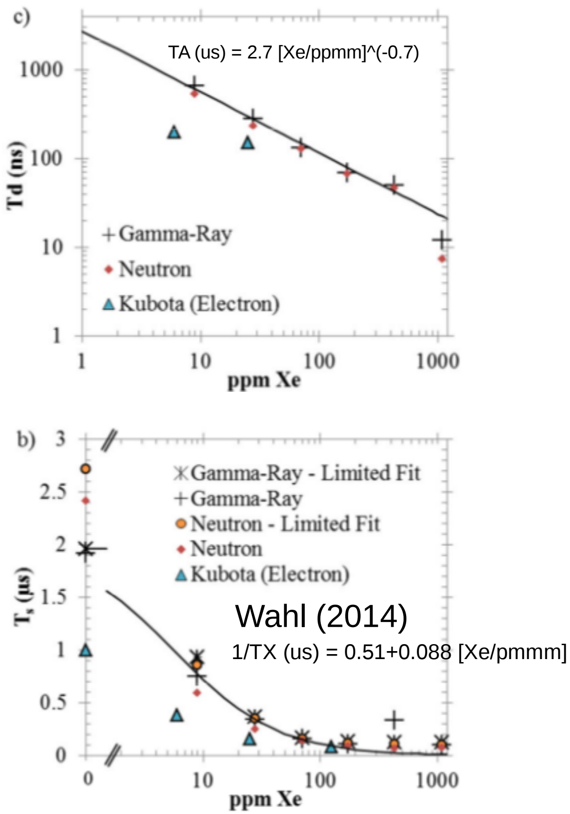


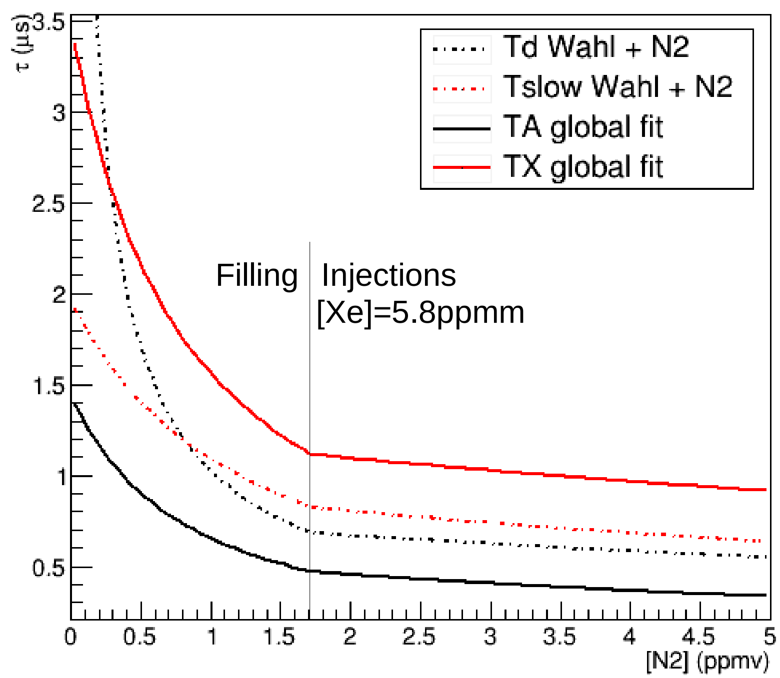


$$\frac{1}{\tau_{TA}} = \frac{1}{\tau_{128}} + \frac{1}{\tau_{N2}} + \frac{1}{\tau_{AX}}$$

$$\frac{1}{\tau_{TX}} = \frac{1}{\tau_{150}} + \frac{1}{\tau_{N2}} + \frac{1}{\tau_{XX}}$$

Probably it is not a good idea to extrapolate Td at low Xe concentrations...

# Backup

# Global fit to 1 TPB-PMT:

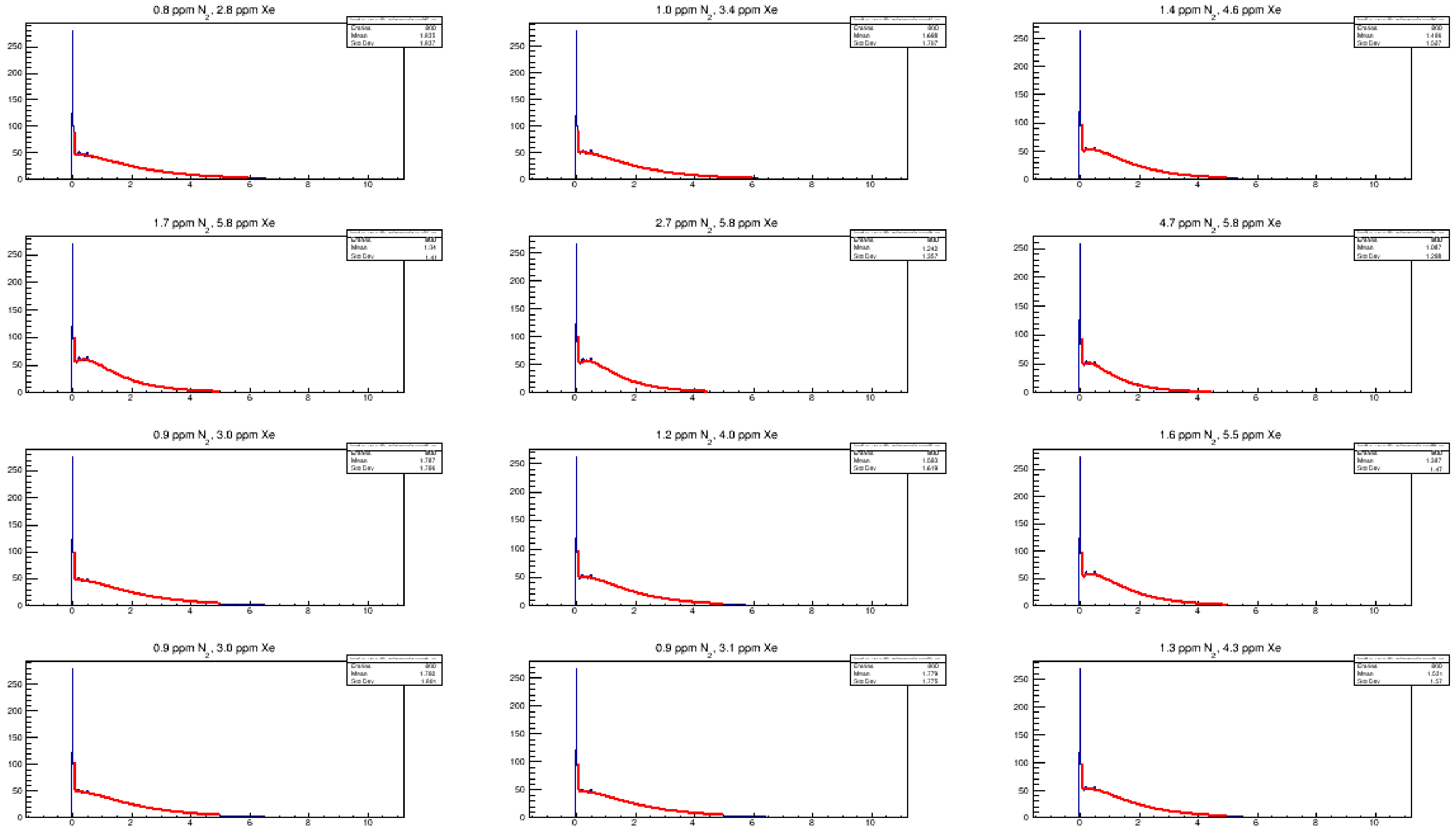

# Impact on the shape
# Comparing with the literature
# Xenon doping

Akimov (2019)

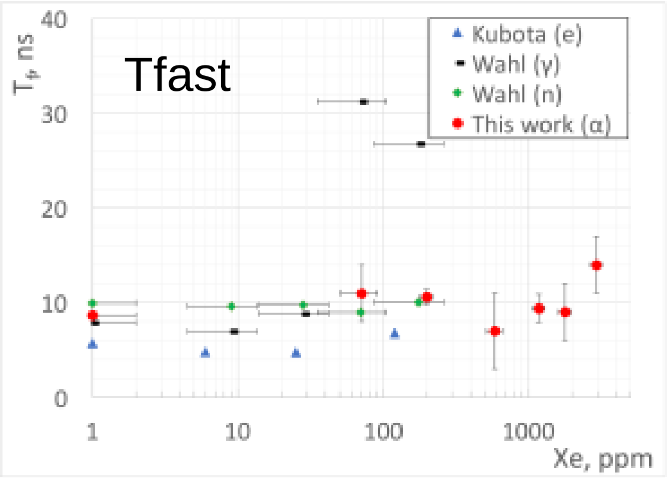


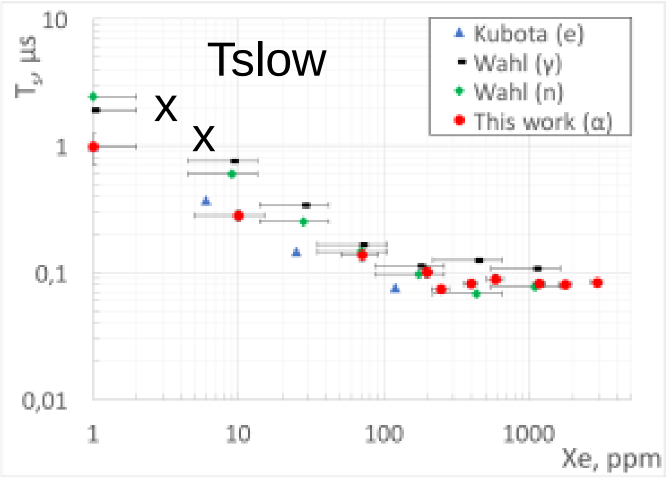


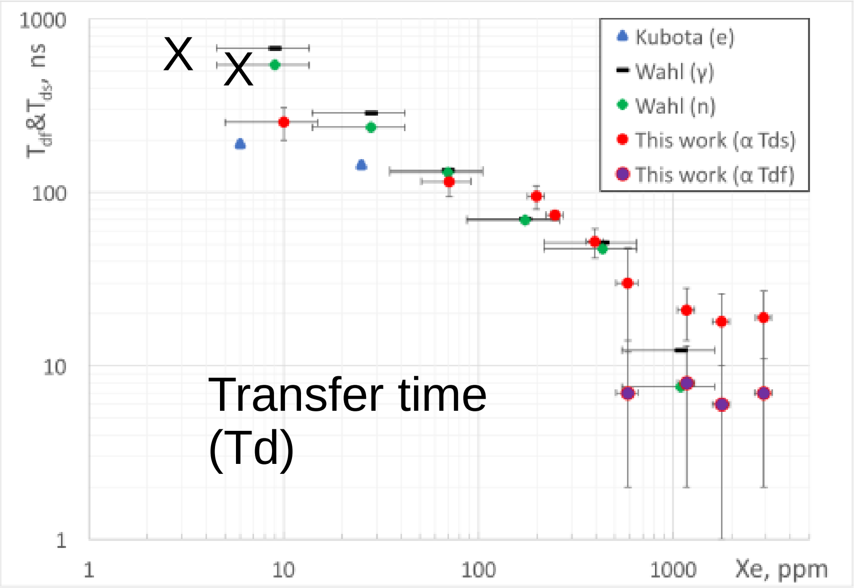


- X's show our values at 3ppm and 6ppm of Xe.
- Values obtained are close to what it is in the literature (without N2!).

# Impact on the shape
# Comparing with the literature
# N2 injections

$$\frac{1}{\tau'_j}([N_2]) = \frac{1}{\tau_j} + k_Q\,[N_2]$$

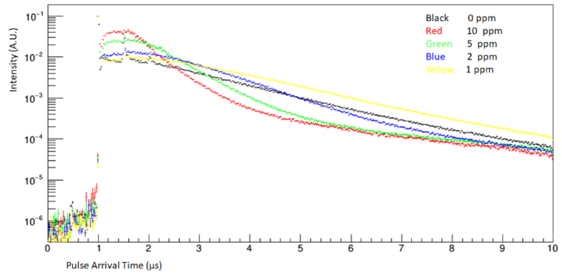


Figure 10: Scintillation distributions created by binning pulse arrival times weighted by the pulse charge for various concentrations of Xe from 0–10 ppm. Distributions are normalized and then scaled to have the same maximum value.

McFadden et al. did a similar measurement, adding N2 to Xenon-doped LAr (at 10ppm).
We used 6ppm.

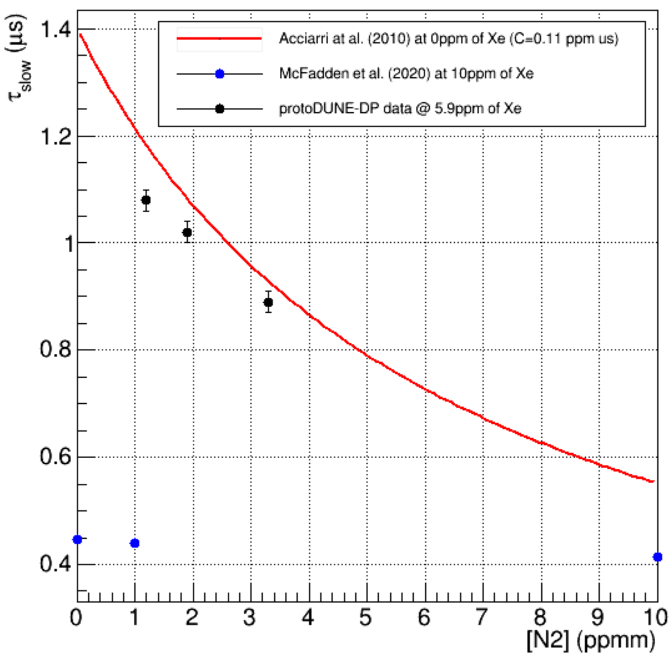


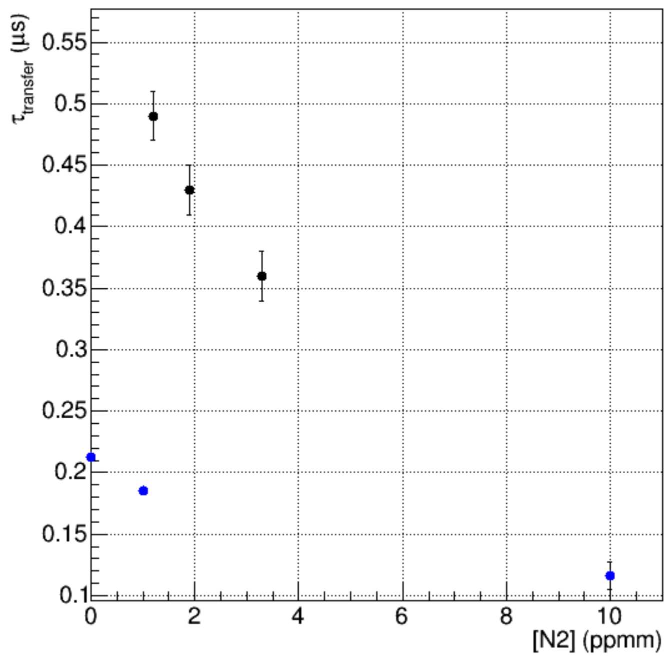

**REFERENCES**


- [1] S. Kubota, M. Hishida, S. Himi, J. Suzuki and J. Ruan, The suppression of the slow component in xenon-doped liquid argon scintillation, Nuclear Instruments and Methods in Physics Research Section A: Accelerators, Spectrometers, Detectors and Associated Equipment 327 (1993) 71–74.

- [2] C. G. Wahl, E. P. Bernard, W. H. Lippincott, J. A. Nikkel, Y. Shin and D. N. McKinsey, Pulse-shape discrimination and energy resolution of a liquid-argon scintillator with xenon doping, JINST 9 (2014) P06013

- [3] D. Akimov et al., Fast component re-emission in Xe-doped liquid argon, JINST 14 (2019) P09022—P09022

- [4] N. McFadden et al., Large-Scale, Precision Xenon Doping of Liquid Argon, arXiv:2006.09780v1 (2020)

# Waves in the tale of the waveform:

Amplitude is proportional to the singal amplitude, and they do not depend on the WLS:

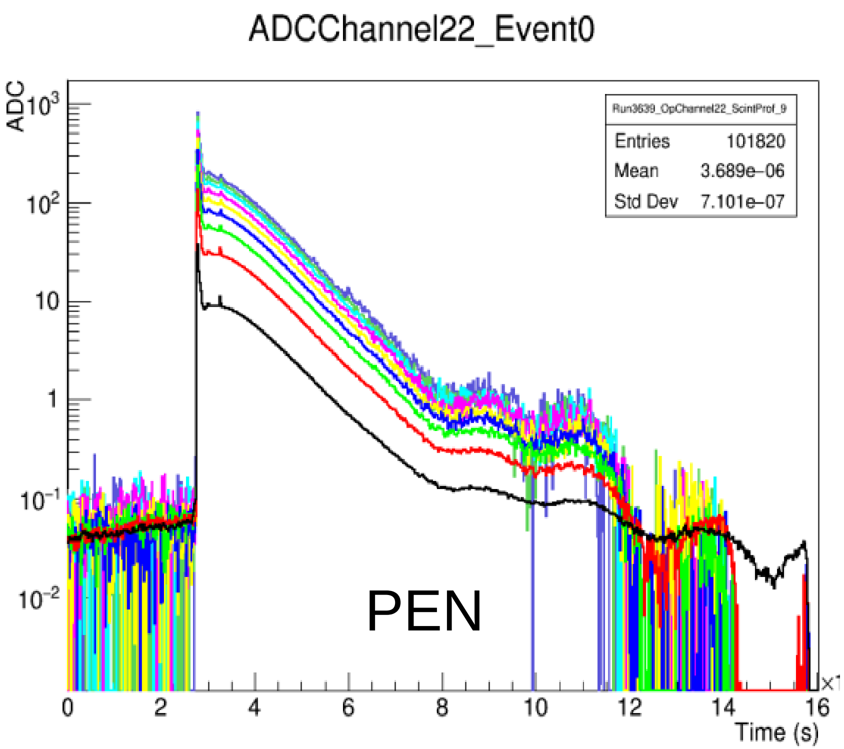


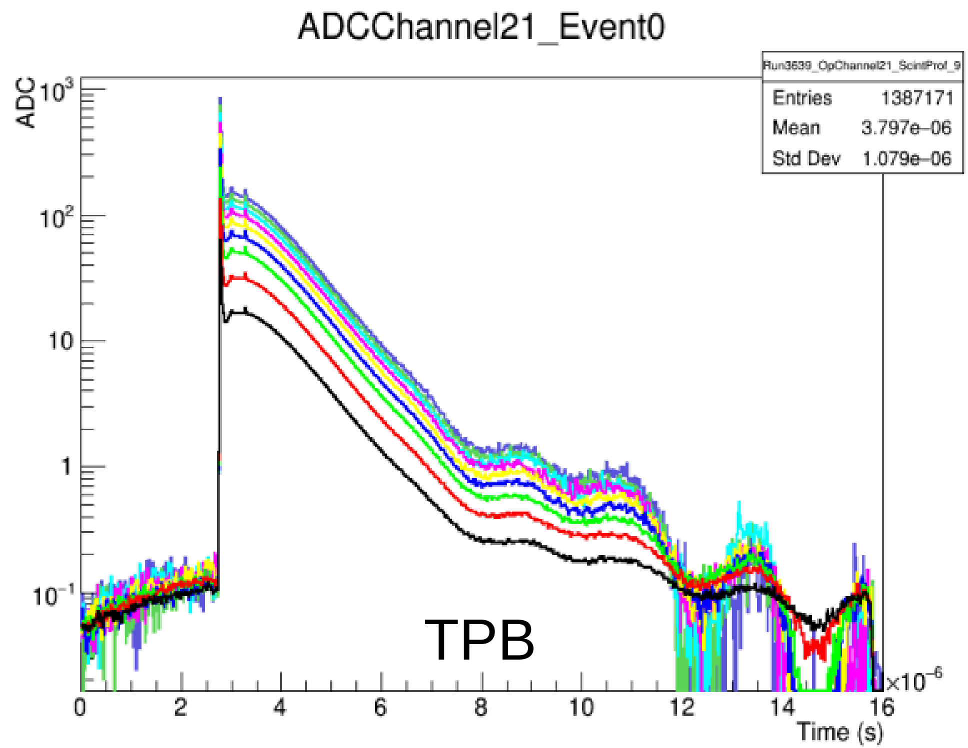


100ADC steps

# Waves in the tale of the waveform:

Amplitude is proportional to the singal amplitude, and they do not depend on the WLS:

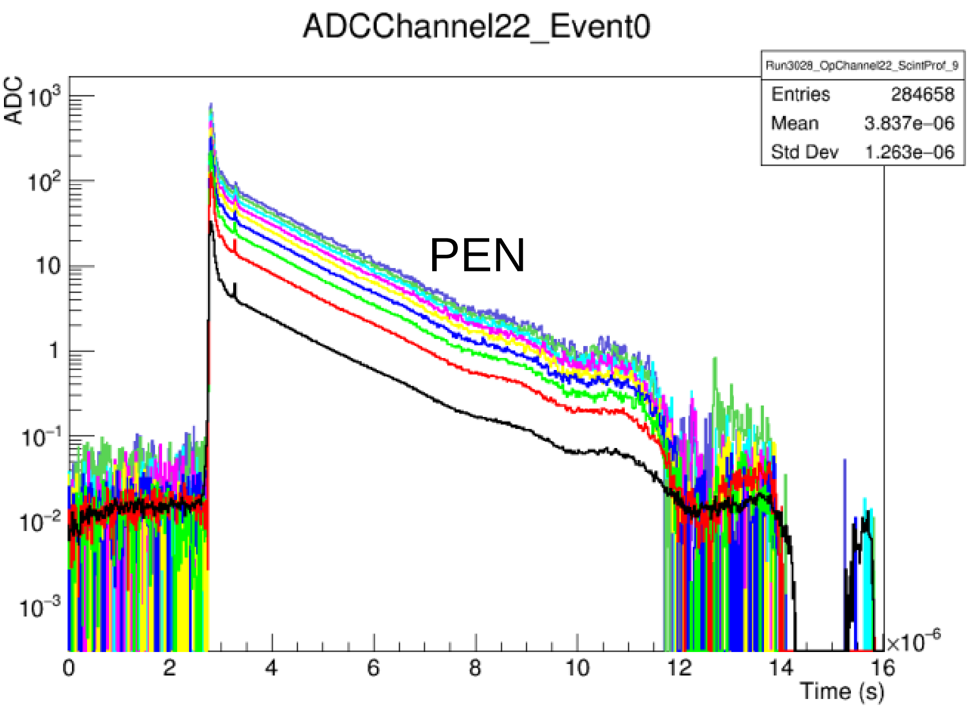


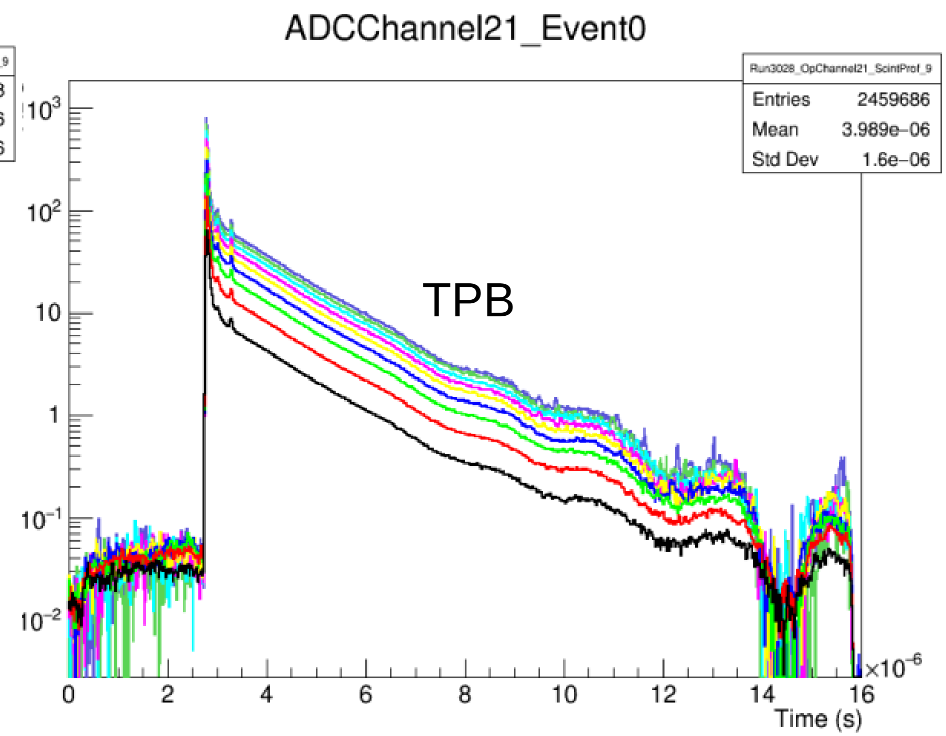


100ADC steps

A. Neumeier et al 2015 EPL109 12001

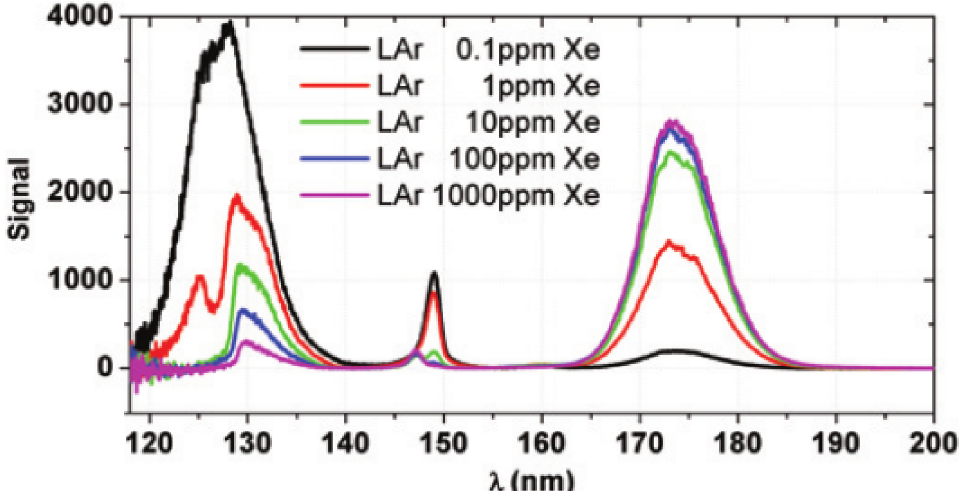


At low Xe concentrations (which is our case), we have a significant contribution at 150 nm.

3 contributions:
128, 147 and 175nm

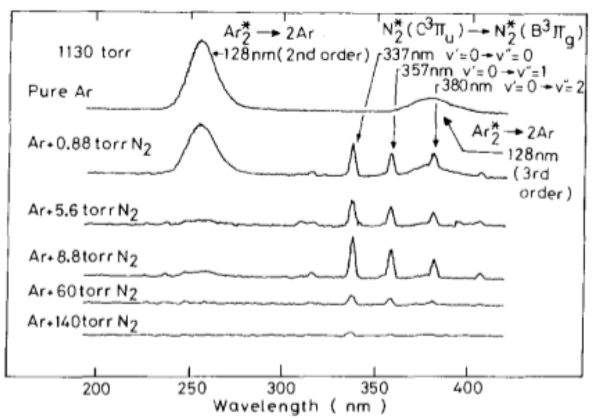


Fig. 3. Emission spectra from a nitrogen/argon gas proportional scintillation counter. The applied voltages are 2500 V for pure argon gas and 0.88 Torr $N_2$ and 2400 V for 5.6 Torr $N_2$ and 2900 V for 60 Torr and 140 Torr $N_2$. The general rise in intensity from 360 to 420 nm is due to third order reflection.

TAKAHASHI et al. (1982)

Also infrared light has been observed (not seen by our PMTs).

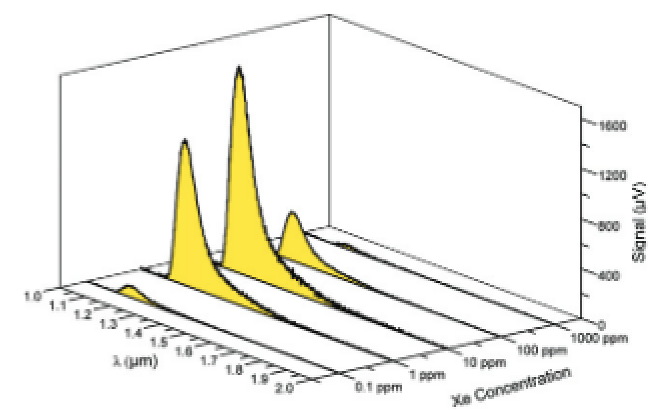


N2 also introduces some peaks at 350nm.

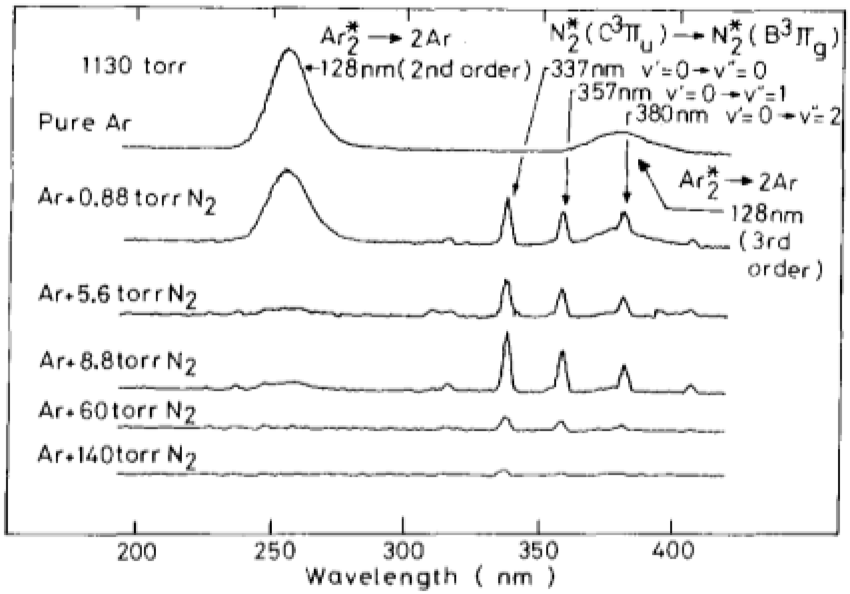


Fig. 3. Emission spectra from a nitrogen/argon gas proportional scintillation counter. The applied voltages are 2500 V for pure argon gas and 0.88 Torr $N_2$ and 2400 V for 5.6 Torr $N_2$ and 2900 V for 60 Torr and 140 Torr $N_2$. The general rise in intensity from 360 to 420 nm is due to third order reflection.

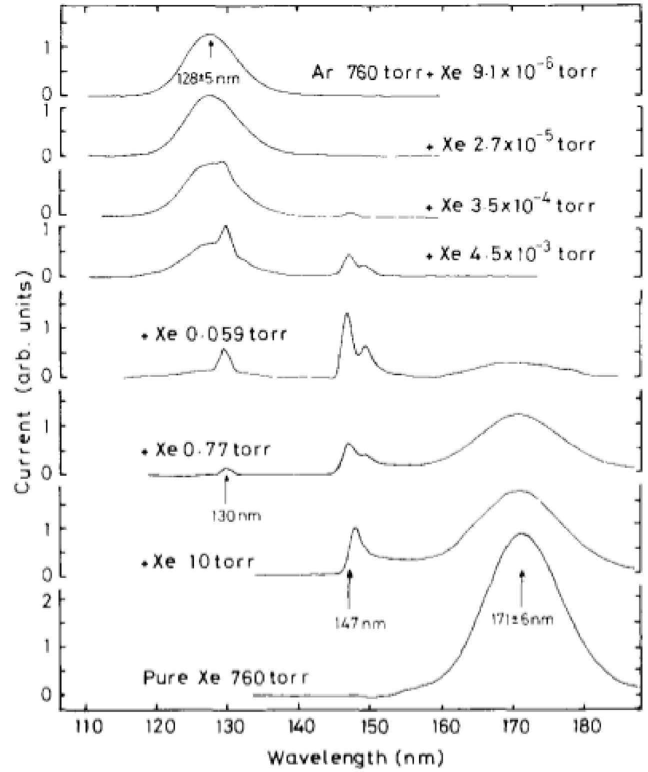


Fig. 1. Emission spectra from a xenon/760 Torr argon gas proportional scintillation counter with an applied voltage of 1600–1900 V.

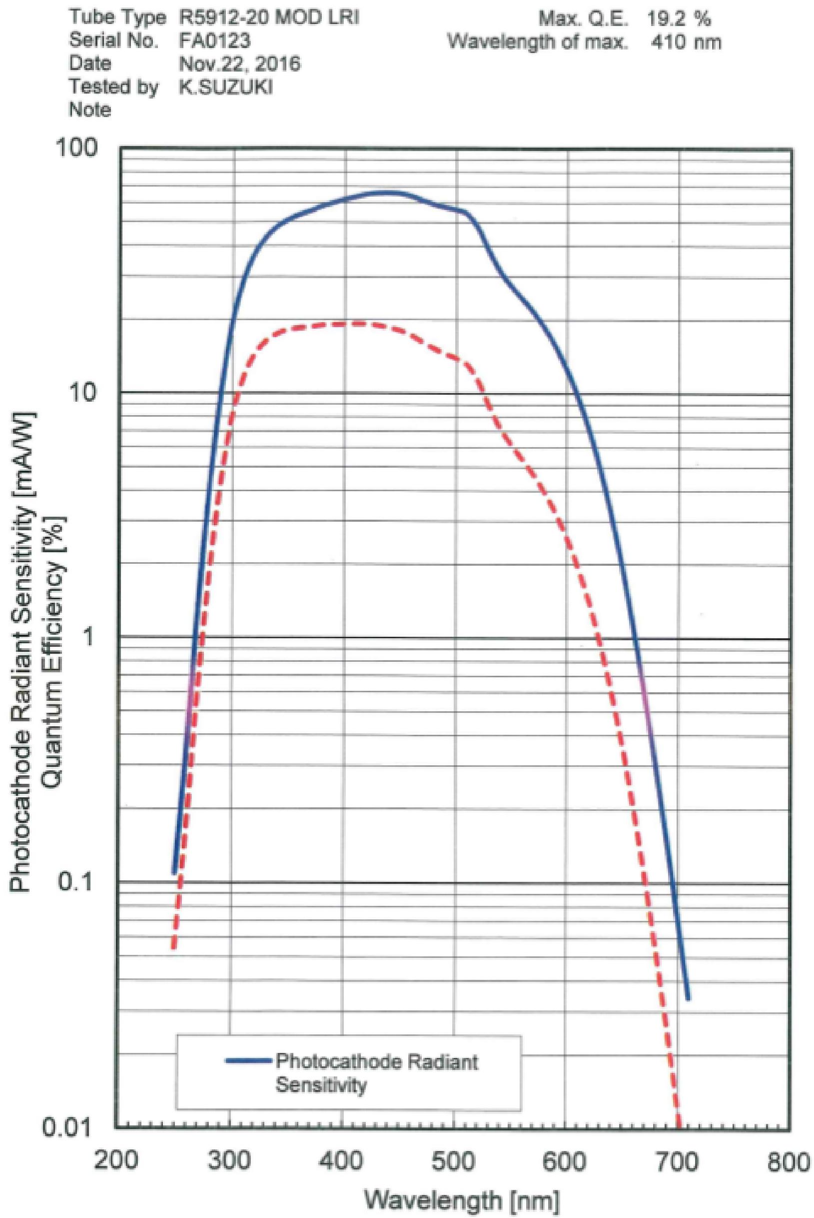


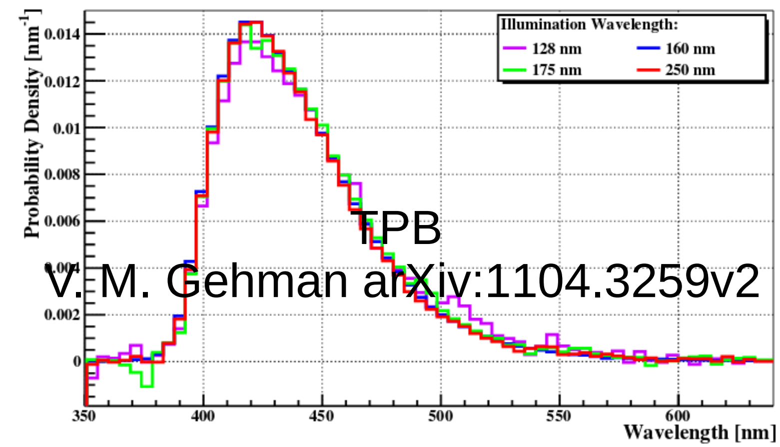


TPB
V. M. Gehman arXiv:1104.3259v2

Figure 7: Visible re-emission spectrum for a TPB film illuminated with 128, 160, 175, and 250 nm light. All spectra are normalized to unit area.

Same TPB emission for all lights!

# Impact on the shape
# What is expected?

McFadden https://www.researchgate.net/publication/342258403_Large-Scale_Precision_Xenon_Doping_of_Liquid_Argon

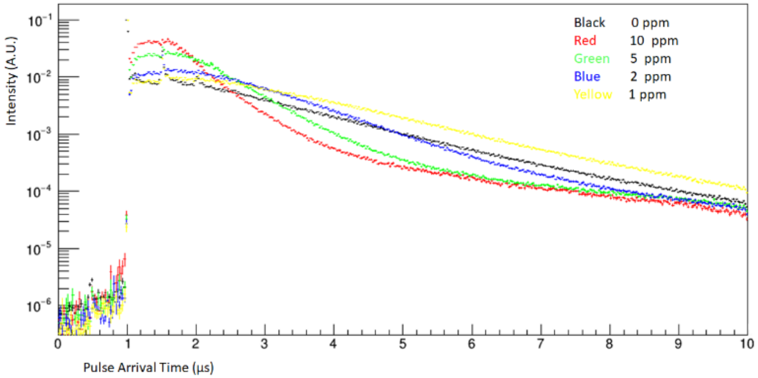


At 1 ppm of $N_2$ and 10 ppm of Xe in LAr, the muon peak from a double coincidence trigger was found to shift from 604.8±6.4 PE to 542±4 PE, which corresponds to 10.4±1.0% reduction in light. This drop in un-doped LAr was measured to be 15.3±3.1%. In 10 ppm $N_2$ and 10 ppm XeDLAr the muon peak shifts to 294±3 PE, a 51.4±0.7% decrease in light yield. A similar drop in light yield is seen in pure LAr when 10 ppm of $N_2$ is injected [23].

N2 quenching:
0.12±0.02 ppm −1 μs −1

| Xenon Doping Time Constants | | | |
|---|---|---|---|
| Concentration | $\tau_s$ (ns) | $\tau_d$ (ns) | $\tau_{long}$ (ns) |
| 1 ppm | 1243±7±6 | 871±10±4 | 3532±212±117 |
| 2 ppm | 771±12±1 | 721±11±1 | 3285±4±5 |
| 5 ppm | 503±11±1 | 435±9±1 | 3415±3±19 |
| 10 ppm | 447±1±2 | 213±4±2 | 2732±4±14 |

attenuation length of 175 nm light in XeDLAr is much longer than the
attenuation length at 128 nm

| Xenon Doping Time Constants | | | |
|---|---|---|---|
| $N_2$ Concentration | $T_s$ (ns) | $T_d$ (ns) | $T_{long}$ (ns) |
| 0 ppm | 447±1±2 | 213±4±2 | 2732±4±14 |
| 1 ppm | 439±1±1 | 185±3±2 | 2408±3±2 |
| 10 ppm | 415±1±1 | 116±11±12 | 2321±4±14 |

Table 3: Summary of xenon doping time constants (ns) for 10 ppm XeDLAr and various concentrations of $N_2$.

| Run | N2 | Xe | #tau_{slow} (us) | #tau_{transfer} (us) |
|---|---|---|---|---|
| 3028 | 0.0 | 0.0 | 1.44±0.03 | - |
| 3320 | 0.2 | 0.6 | 3.34±0.08 | - |
| 3330 | 0.3 | 1.0 | 3.09±0.07 | - |
| 3340 | 0.8 | 2.8 | 1.71±0.04 | 0.70±0.03 |
| 3350 | 1.0 | 3.4 | 1.53±0.03 | 0.62±0.04 |
| 3357 | 1.3 | 4.6 | 1.25±0.02 | 0.57±0.02 |
| 3510 | 1.7 | 5.9 | 1.08±0.02 | 0.49±0.02 |
| 3542 | 2.7 | 5.9 | 1.02±0.02 | 0.43±0.02 |
| 3639 | 4.6 | 5.9 | 0.89±0.02 | 0.36±0.02 |

# Photon emission and atomic collision processes in two-phase argon doped with xenon and nitrogen

A. BUZULUTSKOV[1,2]

[1] *Budker Institute of Nuclear Physics SB RAS, Novosibirsk, 630090, Russia*
[2] *Novosibirsk State University, Novosibirsk, 630090, Russia*



PACS 95.55.Vj – Neutrino, muon,pion, and other elementary particle detectors; cosmic ray detectors
PACS 61.25.Bi – Liquid noble gases
PACS 95.35.+d – Dark matter

**Abstract** –We present a comprehensive analysis of photon emission and atomic collision processes in two-phase argon doped with xenon and nitrogen. The dopants are aimed to convert the VUV emission of pure Ar to the UV emission of the Xe dopant in the liquid phase and to the near UV emission of the $N_2$ dopant in the gas phase. Such a mixture is relevant to two-phase dark matter and low energy neutrino detectors, with enhanced photon collection efficiency for primary and secondary scintillation signals. Based on this analysis, we show that the recently proposed hypothesis of the enhancement of the excitation transfer from Ar to $N_2$ species in the two-phase mode is either incorrect or needs assumption about a new extreme mechanism of the excitation transfer coming into force at lower temperatures, in particular that of the resonant excitation transfer via $ArN_2$ compound (van der Waals molecule).

# Effect of N2 in LAr

$k_Q(N_2) = 0.11 \pm 0.01\ \mu s^{-1} ppm^{-1}$ (volume)

$$\frac{1}{\tau'_j}([N_2]) = \frac{1}{\tau_j} + k_Q\,[N_2]$$

$$A'_j([N_2]) = \frac{A_j}{1+\tau_j\,k_Q\,[N_2]}$$

Expected:

| N2 concentration | | | |
|---|---|---|---|
| in vol. | in mass | tau slow | Aslow |
| 0 | 0 | 1.40 | 1.00 |
| 1.7 | 1.2 | 1.18 | 0.84 |
| 2.7 | 1.9 | 1.08 | 0.77 |
| 4.7 | 3.3 | 0.93 | 0.66 |